



OPEN ACCESS

EDITED BY

Anne S. Meyer,
Technical University of Denmark,
Denmark

REVIEWED BY

Vishal Kumar,
Yeungnam University, South Korea
Pratyosh Shukla,
Banaras Hindu University, India

*CORRESPONDENCE

Hua Yin,
yinhua@tsingtao.com.cn
Lushan Wang,
lswang@sdu.edu.cn

SPECIALTY SECTION

This article was submitted to Industrial
Biotechnology,
a section of the journal
Frontiers in Bioengineering and
Biotechnology

RECEIVED 10 May 2022

ACCEPTED 02 August 2022

PUBLISHED 26 August 2022

CITATION

Wu X, Shi Z, Tian W, Liu M, Huang S,
Liu X, Yin H and Wang L (2022), A
thermostable and CBM2-linked
GH10 xylanase from *Thermobifida fusca*
for paper bleaching.
Front. Bioeng. Biotechnol. 10:939550.
doi: 10.3389/fbioe.2022.939550

COPYRIGHT

© 2022 Wu, Shi, Tian, Liu, Huang, Liu, Yin
and Wang. This is an open-access article
distributed under the terms of the
[Creative Commons Attribution License
\(CC BY\)](https://creativecommons.org/licenses/by/4.0/). The use, distribution or
reproduction in other forums is
permitted, provided the original
author(s) and the copyright owner(s) are
credited and that the original
publication in this journal is cited, in
accordance with accepted academic
practice. No use, distribution or
reproduction is permitted which does
not comply with these terms.

A thermostable and CBM2-linked GH10 xylanase from *Thermobifida fusca* for paper bleaching

Xiuyun Wu^{1,2,3}, Zelu Shi³, Wenya Tian³, Mengyu Liu³,
Shuxia Huang², Xinli Liu¹, Hua Yin^{2*} and Lushan Wang^{3*}

¹State Key Laboratory of Biobased Material and Green Papermaking, Qilu University of Technology, Shandong Academy of Sciences, Jinan, China, ²State Key Laboratory of Biological Fermentation Engineering of Beer, Qingdao, China, ³State Key Laboratory of Microbial Technology, Institute of Microbial Technology, Shandong University, Qingdao, China

Xylanases have the potential to be used as bio-deinking and bio-bleaching materials and their application will decrease the consumption of the chlorine-based chemicals currently used for this purpose. However, xylanases with specific properties could act effectively, such as having significant thermostability and alkali resistance, etc. In this study, we found that *TfXyl10A*, a xylanase from *Thermobifida fusca*, was greatly induced to transcript by microcrystalline cellulose (MCC) substrate. Biochemical characterization showed that *TfXyl10A* is optimally effective at temperature of 80 °C and pH of 9.0. After removing the carbohydrate-binding module (CBM) and linker regions, the optimum temperature of *TfXyl10A*-CD was reduced by 10 °C (to 70 °C), at which the enzyme's temperature tolerance was also weakened. While truncating only the CBM domain (*TfXyl10AdC*) had no significant effect on its thermostability. Importantly, polysaccharide-binding experiment showed that the auxiliary domain CBM2 could specifically bind to cellulose substrates, which endowed xylanase *TfXyl10A* with the ability to degrade xylan surrounding cellulose. These results indicated that *TfXyl10A* might be an excellent candidate in bio-bleaching processes of paper industry. In addition, the features of active-site architecture of *TfXyl10A* in GH10 family were further analyzed. By mutating each residue at the -2 and -1 subsites to alanine, the binding force and enzyme activity of mutants were observably decreased. Interestingly, the mutant E51A, locating at the distal -3 subsite, exhibited 90% increase in relative activity compared with wild-type (WT) enzyme *TfXyl10A*-CD (the catalytic domain of *TfXyl10A*). This study explored the function of a GH10 xylanase containing a CBM2 domain and the contribution of amino acids in active-site architecture to catalytic activity. The results obtained provide guidance for the rational design of xylanases for industrial applications under high heat and alkali-based operating conditions, such as paper bleaching.

KEYWORDS

xylanase, glycoside hydrolase family 10, carbohydrate-binding module, active-site architecture, site-directed mutation

Introduction

In recent years, enzymes have been widely used in the pulp and paper industry to ensure environmentally sustainable development, especially in the pulp bleaching process (Gupta et al., 2022). In the bleaching process, biological enzymes can not only reduce the amount of chemical bleaching agent needed to improve the whiteness of paper pulp, but also reduce the content of ionic waste in the bleaching liquid (Kumar et al., 2016; Gupta et al., 2022). Xylanase is a common bleaching agent, which can open the link between cellulose and lignin by degrading the xylan in plant fiber and facilitate the removal of lignin (Walia et al., 2017). Xylanase can improve the bleaching effect of pulp in elemental chlorine free bleaching (ECF) and total chlorine free bleaching (TCF) processes, and the physical properties of pulp can also be further improved (Rencoret et al., 2013). Saleem et al. (2009) reported 15% decrease in chlorine consumption, 26% increase in brightness and 16.2% reduction in kappa number for wood pulp pretreatment with thermostable xylanase from *Bacillus* Sp. XTR-10. In another study, the use of xylanase from *Aspergillus nidulans* with optimum temperature (60 °C) and pH (9.0) could reduce lignin content of bamboo pulp, as shown by the reduced peak intensity and the reduction in kappa number (Khambhaty et al., 2018). One of the limitations of xylanase application in bio-bleaching is that these enzymes should be both thermostable and alkaline-stable (Kumar et al., 2016; Talens-Perales et al., 2020). Previous studies have reported the application of a xylanase (XynG1-1R) from *Paenibacillus campinasensis* G1-1 (optimal activity at 60°C and pH 7.0) and xylanase A from *Bacillus halodurans* C-125 (optimal activity at 70°C and pH 9.0) on bio-bleaching of pulp and paper (Zheng et al., 2012; Lin et al., 2013). Thus, an increasing number of studies are focusing on the identification and generation of xylanases with higher thermal and alkali resistance (optimum temperature above 60°C, optimum pH above 7.0) and that this is a major biotechnological goal in the pulp and paper industry.

Xylanases (EC 3.2.1.8) are a group of enzymes that hydrolyze the β -1,4 bond in the xylan backbone. According to the CAZy database (<http://www.cazy.org>), xylanases are classified within a number of glycoside hydrolase (GH) families, with the vast majority of characterized xylanases belonging to GH10 and GH11 families (Lombard et al., 2013). The GH11 xylanases usually possess only a catalytic domain (Miao et al., 2017) and may contain secondary binding site on their surface (Ludwiczek et al., 2007). In contrast, most GH10 xylanases contain carbohydrate binding modules (CBMs) (Ali et al., 2005; Guillén et al., 2010). Recent studies have shown that CBMs apparently exhibit substrate specificities, such as CBM 1, 2a, 3, 5, and 10 have affinity for crystalline cellulose, while CBM 2b, 4, 6, 13, 15, and 22 specifically bind to xylan substrates (Boraston et al., 2004; Guillén et al., 2010). The catalytic activity of xylanase was

increased by fusing XynB from *Thermotoga Maritima* with CBM2 (Kittur et al., 2003), while the addition of CBM6 and CBM22 to xylanase Z of *Clostridium thermocellum* resulted in decreased activity and facilitated activity, respectively (Khan et al., 2013). Meng et al. (2015) reported that CBM was crucial to enzymatic activity and thermostability of GH10 XynB from *Caldicellulosiruptor* sp. F32 through truncation experiments. In addition, since the active site architectures of GH10 and GH11 xylanases were different, substituted xylose residues could locate at +1 and -3 subsites in GH10 family xylanases but at the +2 subsite in GH11 family xylanases (Pell et al., 2004; Pollet et al., 2009; Gong et al., 2016).

Thermobifida fusca, a cellulolytic bacterium, possesses excellent physiological and biochemical characteristics, such as thermostability, high activity and wide pH tolerance (Gomez del Pulgar and Saadeddin, 2014). *T. fusca* can efficiently degrade cellulosic biomass by secreting a variety of glycoside hydrolases, such as cellulase, xylanase, arabinofuranosidase, mannanase, 1,3- β -glucanase (Gomez del Pulgar and Saadeddin, 2014). Among these enzymes, three xylanases have been discovered, namely Xyl10A and Xyl10B of the GH10 family and Xyl11A of the GH11 family. A previous functional proteomic study found that GH11 xylanase derived from *T. fusca* was mainly induced by xylan substrates, while GH10 xylanase was mainly induced by microcrystalline cellulose (MCC) substrate (Shi et al., 2020). Xyl10B and Xyl11A had been purified and characterized, and the latter was shown to act more effectively on xylan, although it was less active than Xyl10B on corn fiber (Kim et al., 2004; Zhao et al., 2015). In addition, three endoxylanases (Xyl10A, Xyl10B and Xyl11A) and one xylosidase (Xyl43A) from *T. fusca* were designed as an artificial cellulosome, which could effectively hydrolyze the wheat straw substrate (Morais et al., 2011). However, the function and characterization of Xyl10A have not been explored in detail. The CBM domain of Xyl10A could bind crystalline regions, helping GH10 xylanases to hydrolyze washed corncob particles (WCCP) rather than pure xylan (Inoue et al., 2015; Miao et al., 2017).

In the present study, we investigated the structure and function of a multi-domain xylanase (*Tf*Xyl10A) obtained from *T. fusca*, in order to exploit a candidate enzyme for bio-bleaching process. The domain truncation experiment was to explore the role of each domain of the enzyme. Moreover, the abilities to hydrolyze different pretreated corn stovers and bind to cellulose and xylan substrates were determined to elucidate the catalytic specificity of *Tf*Xyl10A and different truncated mutants. Structural bioinformatics analysis and an alanine-scanning experiment of the active-site architecture were performed to better comprehend structural basis of catalytic activity of GH10 xylanases. This study will contribute to understanding the function and catalytic mechanism of a thermo-alkali xylanase, and provide guidance for the rational design and industrial application of enzymes belonging to the GH10 family.

Materials and methods

Strains and cultivation conditions

Thermobifida fusca DSM43792 (Genebank accession no. AF002264) was purchased from Deutsche Sammlung von Mikroorganismen und Zellkulturen (DSMZ, Braunschweig, Germany). A 0.5% (v/v) inoculant was used for cells growth in Czapek's medium at 55°C and the culture was shaken at 200 rpm for 20 h. The medium was centrifuged at $\times 5000$ g for 2 min to collect cells, followed by washing two times using sterile water. Then, these cells were transformed into fresh Czapek's mediums with 1% (w/v) of xylan or microcrystalline cellulose (MCC) as the sole induced carbon source. The cells were harvested at different sampling time (0, 2, 6, and 12 h) by centrifuging at $\times 5000$ g for 2 min and then stored at -80°C .

Escherichia coli DH5 α and BL21 (DE3) (Dingguo, Beijing, China) were used for molecular cloning and secretory expression of xylanases, respectively. All *E. coli* strains were grown in Luria-Bertani (LB). The Blunt-E1 plasmid (Transgen, Beijing, China) was used as the expression vector.

RNA isolation and quantitative PCR

Bacteria samples at different time points were used to extract RNA and synthesize cDNA. Total RNA was extracted using the TRIzol method (Rio et al., 2010). And the integrity of RNA was confirmed by 1% (w/v) agarose gel electrophoresis. The cDNA was synthesized using an Evo M-MLV reverse transcription kit (AG, China) according to the manufacturer's protocol. The concentration and purity of cDNA were determined by measuring UV absorbance with the Nanophotometer[®] N60 (Implen, Munich, Germany). The qPCR was carried out using power SYBR[®] Green Pro Taq HS (AG, China) in qTOWER³G (Analytic Jena, Jena, Germany). The primers used to detect the transcriptional levels of encoding genes are listed in Supplementary Table S1. The target genes included three xylanase genes (*xyl11a*, AHK22788.1; *xyl10a*, AAZ56956.1; *xyl10b*, AAZ56824.1). The gyrase gene (*gyra*, AAZ54047.1) was used as an internal reference gene. The transcription of all target genes were normalized relative to the *gyra* gene. Three biological replicates and three experiment replicates were performed for each sample.

Plasmid construction

The genes, encoding the *TfXyl10A*, *TfXyl10AdC* (catalytic domain + linker), and *TfXyl10A-CD* (only catalytic domain), were amplified from the genomic DNA of *T. fusca* DSM10635 and cloned into the vector Blunt-E1 to obtain recombinant plasmids. The gene encoding *TfXyl10A-CD* was

used as the wild-type (WT) and site-directed mutagenesis was performed using a PCR-based method (Weiner et al., 1994). A PCR was performed (S1000 Thermal Cycler; Bio-Rad, Hercules, CA, United States) using PrimeSTAR Max Premix (TaKaRa, Shiga, Japan). The sequences of primers used for expression and mutagenesis are listed in Supplementary Table S2. After digesting with *DpnI* (ABclonal Biotech, Wuhan, China) and fragment purification, the PCR product was transformed into *E. coli* DH5 α using LB-ampicillin plates. Plasmid recovery was conducted using a GV-plasmid DNA mini extraction kit (Dingguo, Beijing, China) followed by sequencing (Tsingke, Qingdao, China) to verify the mutations. All constructed recombinant plasmids contained an N-terminal His₆ tag.

Protein expression and purification

The correct recombinant plasmids were further transformed into *E. coli* BL21 (DE3) to produce recombinant proteins induced by 1 mM isopropyl β -D-thiogalactopyranoside (IPTG, Sangon Biotech, Shanghai, China) for 20 h at 20°C. *E. coli* BL21 (DE3) cells were harvested by centrifugation and resuspended in pH 8.0 NaH₂PO₄/NaCl buffer (50 mM NaH₂PO₄ and 300 mM NaCl). Ultrasonic Homogenizer (JY92-IIDN, SCIENTZ, Ningbo, China) was used for cell fragmentation. The method was to use 20 kHz frequency, 200 W power, each crushing 30 s, 30 s interval, repeated crushing 30 min at 4°C. After ultrasonic fragmentation, the recombinant proteins were purified with Ni Sefinose[™] 6 Fast Flow (GE Healthcare Bio-Science AB, Uppsala, Sweden). The samples were applied to the column by gravity flow. First, the column was equilibrated with 10 ml pH 8.0 NaH₂PO₄/NaCl buffer with 5 mM imidazole. Subsequently, after the sample has entered the resin, the column was washed with 20 ml of washing buffer (50 mM NaH₂PO₄ and 300 mM NaCl, 20 mM imidazole; pH 8.0) to remove nonspecifically bound proteins. Then, 10 ml of elution buffer (50 mM NaH₂PO₄ and 300 mM NaCl, 100 mM imidazole; pH 8.0) and 10 ml of elution buffer (50 mM NaH₂PO₄ and 300 mM NaCl, 250 mM imidazole; pH 8.0) were used to collect target proteins. The purified proteins were analyzed by sodium dodecyl sulfate-polyacrylamide gel electrophoresis (SDS-PAGE). The protein marker was enhanced 3-color regular range protein marker with the segments range of 10–180 KDa (PM2510, SMOBIO Technology, Inc.). The protein concentration was measured by the Bradford method with bovine serum albumin as the standard (Bradford, 1976).

Enzymatic properties assays

Xylanase activity was measured by the dinitrosalicylic (DNS) acid method (Miller, 1959). For detection of the optimal temperature, 0.25 μM of the purified enzymes was mixed with

1% xylan at different temperatures ranging from 30°C to 90°C in sodium citrate buffer (pH 7.0) for 10 min. The optimal pH of xylanases was determined in the range of pH 3.0–11.0 (50 mM sodium citrate buffer, pH 3.0–8.0; 50 mM Glycine-NaOH buffer, pH 9.0–10.0; Na₂HPO₄-NaOH buffer, pH 11.0) using beechwood xylan (BX) substrate for 10 min at 80°C. Thermostability of xylanases was measured by evaluating the residual activity (Han et al., 2020) at the optimum pH 9.0 after preincubating for 60 min at different temperatures ranging from 30°C to 90°C. In addition, xylanases were preincubated at 80°C for different time intervals (0, 5, 15, 30, and 60 min) and the residual activities were also determined under the optimum reaction conditions (80°C and pH 9.0). And we detected pH stability of xylanases by assessing the residual activity under the optimum reaction conditions (80°C and pH 9.0) after incubation at pH 9.0 for 0, 5, 15, 30 and 60 min. After enzyme and substrate mixed reaction, 80 µL of DNS solution was added and then the solution was boiled for 10 min immediately to terminate the reaction. After adding 820 µL deionized water, the absorbance was detected at a wavelength of 550 nm by an ultraviolet spectrophotometer (Puyuan Instruments, Ltd., Shanghai, China). One unit of xylanase activity (U) was defined as the amount of enzyme (mg) that released 1 µmol of xylose per minute under the optimal assay conditions.

Hydrolysis of pretreated corn stover

Corn stover was collected from Dezhou, Shandong Province, China. The PCS was prepared as previously reported with a slight modification (Wang et al., 2019). The cleaned corn stover was crushed by a knife mill and subsequently passed through a 30-mesh sieve. The collected corn stover was incubated with 15% of aqueous ammonia solution for 12 h at 60°C and washed with deionized water until its pH was neutral. After being oven-dried at 80°C to obtain a constant weight, the solids were used as the substrate named “PCS-1”. The solids were further degraded by *TfXyl11A* to remove long-chain xylan backbone and the resulting substrate with less xylan residue was named “PCS-2”.

Then, 0.5 µM of *TfXyl10A*, *TfXyl10AdC* or *TfXyl10A-CD* was mixed with each substrate. After incubation at 80°C for different time periods, the reducing sugar released from each substrate was detected by the DNS method. Three replicates were performed for each sample.

Measurement of the polysaccharide-binding capacity

Polysaccharide-binding experiments were carried out to clarify the binding characteristics of the CBM2 domain in

TfXyl10A. Two different natural polysaccharides, corncob xylan and MCC, were dissolved in pH 7.0 Na₂HPO₄-citric acid buffer, and were centrifuged at ×14,000 g for 5 min; then the supernatant was discarded. Insoluble solid substrates were collected after five washes. *TfXyl10A*, *TfXyl10AdC* or *TfXyl10A-CD* (400 µL 1 µM) were incubated with each substrate (0.02 g) at 4°C for 1 h. Then the supernatants were collected after ×14,000 g centrifugation for 10 min at 4°C. The residual enzyme activity in the supernatants was measured using BX as a substrate.

Enzyme kinetics

Kinetic analysis of the catalytic reactions were performed under standard conditions using purified enzymes (100 µL) and various concentrations of BX substrates (0.2–10%, 500 µL) for 5 min at 80°C, then 400 µL DNS solution was added to terminate the reaction. The kinetic parameters were nonlinearly fitted based on the Michaelis-Menten equation using Prism 5.0 software (GraphPad, San Diego, CA, United States) (Motulsky, 2007).

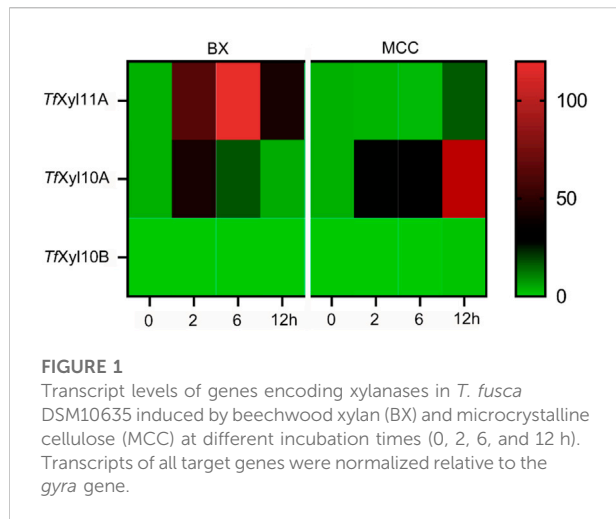
Structural bioinformatic analysis

The sequence and structure information of GH10 xylanases were obtained from the National Center for Biotechnology Information (NCBI, <http://www.ncbi.nlm.nih.gov/>), Uniprot (<http://www.uniprot.org/>), Protein Data Bank (PDB, <http://www.rcsb.org/>), and Carbohydrate-Active enzyme (CAZY, <http://www.cazy.org/Glycoside-Hydrolases.html>). Swiss-model (<http://beta.swissmodel.expasy.org/>) was used to model the 3-D structure of *TfXyl10A* catalytic domain with the template of *CfXyn10A* (PDB 3CUJ). The xylanase *CfXyn10A* (PDB 3CUJ) were used to find the amino acid residues in the active-site architecture of GH10 xylanases. The conservation of the sequence profile was tested by the ConSurf Sever (Haim et al., 2016).

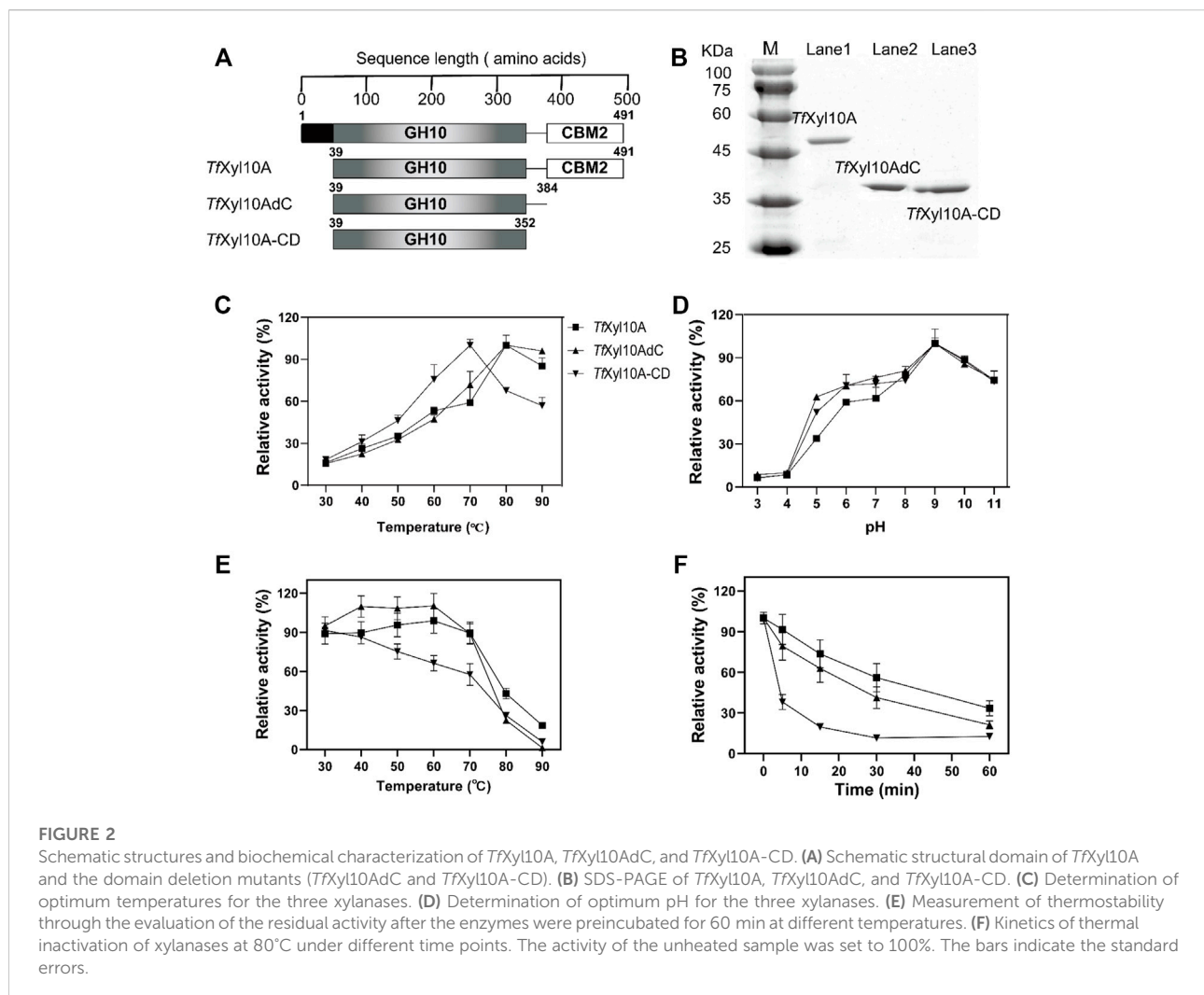
Results

Transcription of the *TfXyl10A* encoding gene induced by microcrystalline cellulose

The genome of *T. fusca* DSM10635 contains three xylanase genes encoding one GH11 xylanase named *TfXyl11A*, and two GH10 xylanases named *TfXyl10A* and *TfXyl10B*. The transcription levels of the three xylanase genes were determined by qPCR with BX or MCC as the sole carbon source. As shown in Figure 1, both genes encoding *TfXyl11A*



and *TfXyl10A* could be induced by BX substrate. Gene encoding *TfXyl11A* showed the highest level of transcription on BX at 6 h. While the amount of *TfXyl10A* transcription increased slightly at 2 h, and then appeared to decrease. However, the transcription level of the gene encoding *TfXyl10A* was lower overall than that of the gene encoding *TfXyl11A*. This might indicate that BX is not the best substrate for inducing to express *TfXyl10A*. Interestingly, the gene encoding *TfXyl10A* also had high transcription levels under MCC induction, with the transcription levels at 12 h being the highest (Figure 1). In addition, the gene encoding *TfXyl10B* was not expressed under either BX or MCC induction, suggesting that it might be a redundant xylanase gene. These results were consistent with previous proteome studies that identified two major xylanases *TfXyl11A* and *TfXyl10A* (Shi et al., 2020).



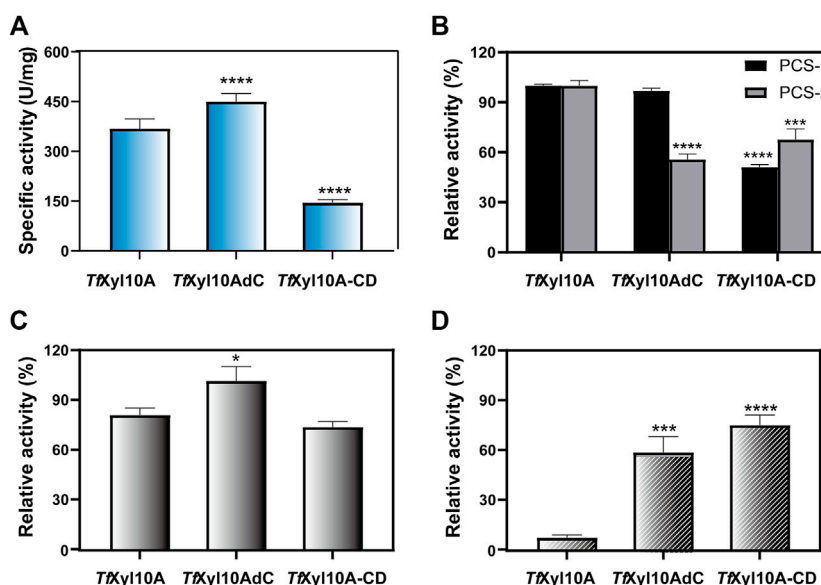


FIGURE 3

Enzyme activities and substrate binding capacities of *TjXyl10A* and the truncation mutants (*TjXyl10AdC* and *TjXyl10A-CD*). (A) Specific activity (U/mg) of *TjXyl10A*, *TjXyl10AdC*, and *TjXyl10A-CD* on beechwood xylan (BX). (B) Relative activity (%) of *TjXyl10A*, *TjXyl10AdC*, and *TjXyl10A-CD* on pretreated corn stover (PCS-1: pretreatment by 15% aqueous ammonia solution; PCS-2: pretreatment by 15% aqueous ammonia solution and hydrolysis of *TjXyl11A*). Enzymatic activity of *TjXyl10A* was defined as 100%. (C) Residual enzyme activities of the supernatants of *TjXyl10A*, *TjXyl10AdC*, and *TjXyl10A-CD* after binding with insoluble solid xylan substrate at 4°C for 1 h. (D) Residual enzyme activities of the supernatants of *TjXyl10A*, *TjXyl10AdC*, and *TjXyl10A-CD* after binding with microcrystalline cellulose (MCC) at 4°C for 1 h. The enzymatic activities of three untreated enzymes was defined as 100%. The bars indicate the standard errors. Three biologically independent replicates were used to calculate means and standard deviations. *p*-values were calculated using Prism by performing one-way ANOVA, with a statistical significance level defined as * ($p < 0.05$), ** ($p < 0.01$), *** ($p < 0.001$), and **** ($p < 0.0001$). Sequence alignment and structural analysis of *TjXyl10A-CD*.

Heterologous expression and enzymatic characterization of *TjXyl10A* and the truncation mutants (*TjXyl10AdC* and *TjXyl10A-CD*)

According to the descriptions in the uniprot database, the complete *TjXyl10A* contained a total of 491 amino acids, including a signal peptide (1–38 amino acids), catalytic domain (CD, 39–352 amino acids) and CBM2 domain (384–491 amino acids). The full-length *TjXyl10A* xylanase and truncation mutants (*TjXyl10AdC* and *TjXyl10A-CD*) were constructed (Figure 2A) and heterologously expressed using the *E. coli* expression system. The purified proteins were examined by SDS-PAGE (Figure 2B). The effects of temperature and pH on enzymatic activity were evaluated using BX as the substrate. As shown in Figure 2C, the optimum temperature of the xylanases *TjXyl10A* and *TjXyl10AdC* was 80°C and more than 80% of the activities were retained at 90°C, while the optimum temperature of *TjXyl10A-CD* was 10°C lower than that of *TjXyl10A* and *TjXyl10AdC*. The thermostability assay showed that *TjXyl10A* and *TjXyl10AdC* preserved more than 88% of the enzyme activity when preincubated at 30–70°C for 60 min, while *TjXyl10A-CD* preserved only 57% at 70°C

(Figure 2E). In addition, *TjXyl10A-CD* incubated at 80°C for 5 min and the enzyme activity was significantly reduced to 38% of the original level (Figure 2F). These results indicated that the linker region is important to maintain the stability of the enzyme structure at high temperatures, but not the CBM domain. The maximum activity of *TjXyl10A*, *TjXyl10AdC* and *TjXyl10A-CD* occurred at pH 9.0 (Figure 2D), with 84% of the relative activity retention under of 9.0 for 60 min incubation (Supplementary Figure S1). These results suggested that *TjXyl10A* is a thermostable and alkaline xylanase, which could be an excellent candidate in industrial applications.

Binding and degradation capacities of *TjXyl10A* and truncated mutants on xylan and cellulose

The specific activity of the recombination enzyme *TjXyl10A* was 368.86 ± 28.85 U/mg on BX. *TjXyl10AdC* had a higher degradation ability than *TjXyl10A* on BX, while the enzyme activity of the mutant *TjXyl10A-CD* was the lowest (Figure 3A). This was consistent with previous reports of GH10 xylanases from *Aspergillus fumigatus* Z5, that is, Xyn10AdC, a CBM1-

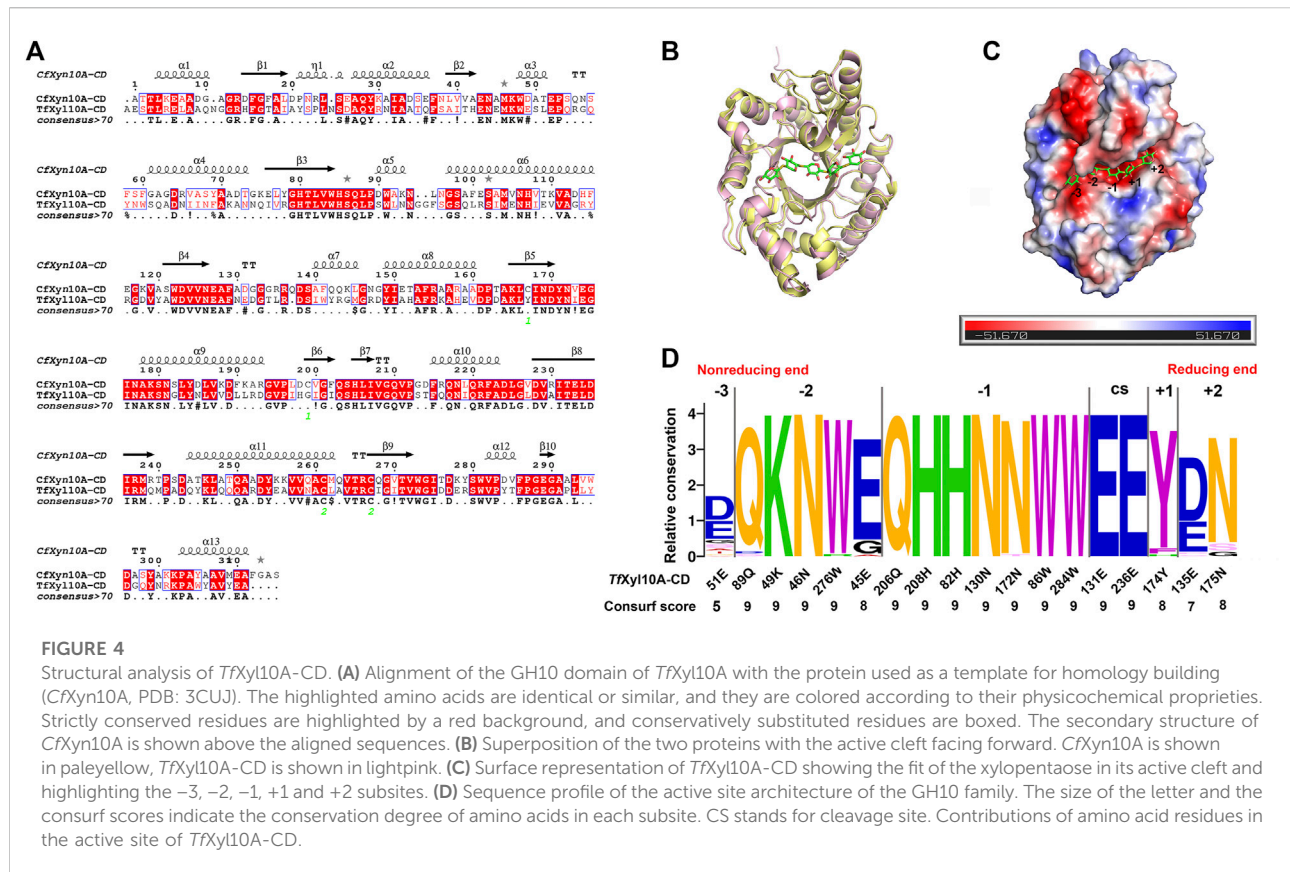
removing mutant, has been reported to have a higher ability to degrade xylan than Xyn10A (Miao et al., 2017). In the degradation of xylan, the linker of *TfXyl10A* was essential for enzyme activity. In addition, the three enzymes showed no significant activities against MCC (data not shown). The enzyme activities of *TfXyl10A*, *TfXyl10AdC*, and *TfXyl10A-CD* were measured using different pretreated corn stover (PCS) samples as substrates (Figure 3B). PCS-1, in which lignin was effectively removed by aqueous ammonia treating (Yoo et al., 2015), mainly contained cellulose and hemicellulose components. PCS-2 was PCS-1 dried sample treated with adequate enzymatic hydrolysis of GH11 family xylanase *TfXyl11A*. PCS-2, in which a large amount of long-chain xylan backbone was effectively degraded (Gong et al., 2016), contained cellulose and xylan residues attached to cellulose surface. The relative activities of *TfXyl10A* and *TfXyl10AdC* were similar, and the relative enzyme activity of *TfXyl10A-CD* was only 50% of the former on PCS-1. This suggested that deletion of both the CBM and linker region severely affects enzyme activity when xylan substrates are abundant, compared with deletion of the CBM domain alone. However, the relative enzyme activity of *TfXyl10AdC* and *TfXyl10A-CD* was significantly lower than that of *TfXyl10A*, when PCS-2 was used as a substrate. These results indicated that *TfXyl10A* could effectively degrade the xylan residues attached to the surface of straw, and CBM2 played an important role. The specific activities of *TfXyl10A*, *TfXyl10AdC* and *TfXyl10A-CD* are shown in Supplementary Table S3.

The substrate affinities of the three enzymes were determined through residual activities analysis after binding. As shown in Figure 3C, after binding with insoluble xylan, the relative residual activity of *TfXyl10A* and *TfXyl10A-CD* on BX decreased by 21.69% and 27.60% compared with their initial enzyme activity and that of *TfXyl10AdC* was almost unchanged, which indicated that compared with *TfXyl10AdC*, *TfXyl10A* and *TfXyl10A-CD* were more tightly bound to insoluble xylan. However, the binding capabilities to MCC were completely different (Figure 3D). *TfXyl10A* supernatant showed the lowest relative residual activity with losing all enzyme activity on BX, compared with *TfXyl10AdC* and *TfXyl10A-CD*. The relative residual activity of supernatants of *TfXyl10AdC* and *TfXyl10A-CD* on BX retained 59.34% and 69.48% of their initial enzyme activity, respectively. *TfXyl10A* containing the CBM2 domain could efficiently bind MCC, indicating that the CBM2 domain played an important role in terms of protein binding to the cellulose substrate. The residual activities of supernatant of *TfXyl10A*, *TfXyl10AdC*, and *TfXyl10A-CD* after binding with insoluble xylan and MCC are shown in Supplementary Table S4.

To better comprehend structural basis of *TfXyl10A-CD* enzymatic activity, we built a 3-D homology model of the enzyme. *CfXyn10A-CD* xylanase from *Cellulomonas fimi* ATCC 484 (PDB: 3CUJ) was used as a structural template.

The sequence alignment of the two proteins is given in Figure 4A, showing a sequence similarity of 54.69%. The conserved regions of the sequences made use of a color code. This conservation was directly reflected in the similarities of their tertiary structures. The two enzymes had a typical TIM α/β -barrel fold with a root-mean-square deviation (RMSD) of 0.549. (Figure 4B). *CfXyn10A-CD* with a sulfur substituted beta-1,4-xylopentose was also used for a detailed structural analysis of the *TfXyl10A-CD* active site. *TfXyl10A-CD* showed a fit with xylopentose in its active site and the -3, -2, -1, +1 and +2 subsites were highlighted (Figure 4C). The sequence profile of the active-site architecture of the GH10 family is shown in Figure 4D, with five and seven amino acid residues centered at the -2 and -1 subsites, respectively. Most of them were conserved across the GH10 family xylanases. There was a total of only four residues located at the subsites -3, +1, and +2. The consurf scores of 51E at -3 subsite was the lowest, "5".

The interaction network between the amino acids of the *TfXyl10A-CD* active site and xyloheptaose was described in Figure 5A. To study the role of active-site residues in the binding of xylopentose, we mutated the residues in the active site to alanine, and the relative activities of the mutants against BX were determined (Figure 5B). The residues Asn-46, Trp-276, His-208, His-82, Trp-86, Glu-131, and Glu-236 were involved in the hydrogen bonding with xylose at subsites -2, -1, and CS, and Trp-284 and Tyr-174 interacted with xylose at subsites -1 and +1 by hydrophobic stacking. This was critical for xylan hydrolysis because the alanine mutants of these residues retained only 10–20% of their activity. The results collectively indicated that the interaction for xyloses at the -2, -1, and +1 subsites were extremely important for xylan catalysis. Only Tyr-174 formed a CH- π hydrophobic interaction with the xylose ring at the +1 subsite, and the O2 and O3 positions of xylose could connect substituents (Figure 5A). The residues Gln-89, Lys-49, and Glu-45 at the -2 subsite and Gln-206, Asn-130 and Asn-172 at the -1 subsite formed a hydrogen bond with xylose, whose mutation to alanine led to approximately half-residual activities. Manipulating the residue Asn-175 at the +2 subsite to alanine also had a slight influence on the enzyme activity of *TfXyl10A-CD*. These results indicated that the interactions with a moderate importance in xylan hydrolysis could be at the subsite distal from the cleavage site. Surprisingly, the relative activity of mutant E51A at the -3 subsite was improved by 90% compared with that of the WT (Figure 5B). The specific activities of WT (*TfXyl10A-CD*) and its variants are shown in Supplementary Table S5. A structural analysis showed that Glu-51 might form an electrostatic interaction with xylose at the -3 subsite, but the interaction force of alanine disappeared after mutation (Supplementary Figure S2). This analysis was consistent with an increase in the kinetic constant k_{cat} , suggesting that the mutant E51A might enhance the product releasing ability to improve the enzymatic activity (Table 1).



Discussion

In this study, we found that one xylanase *TfxYl10A* in *T. fusca* could be induced by the cellulose substrate MCC, while the other two xylanases (*TfxYl11A* and *TfxYl10B*) were not (Figure 1). Previous studies have shown that cellobiose could induce the expression of cellulases, cellulose-binding proteins, and a xylanase *TfxYl10A* (Chen and Wilson, 2007). Deng and Fong (2010) measured the cellulase-related gene expression in WT and *celR*-disrupted *T. fusca* and found that there were no detectable mRNA transcripts of *TfxYl10A* in any of the samples of the *celR* deletion strain, confirming that *CelR* may activate transcription of this gene. The biochemical experiments showed that *TfxYl10A* containing the CBM2 domain could efficiently hydrolyze PCS-2 (Figure 3B) and bind to the MCC substrate (Figures 3C,D), indicating that this CBM had an important role in terms of protein binding to the cellulose substrate. The CBM1 is known to specifically bind to insoluble and highly crystalline cellulose and/or chitin (Gilbert et al., 2013). In a previous study, we also identified a GH10 family xylanase with CBM1 (G0SBF1), which was co-expressed with most cellulolytic enzymes in temporal secretomes and a transcriptional analysis of *Chaetomium thermophilum* (Li et al., 2020). CBMs can potentiate the action of a cognate catalytic module toward polysaccharides in intact cell

walls through the recognition of nonsubstrate polysaccharides, which explains why cellulose-directed CBMs are appended to many noncellulases (Herve et al., 2010; Inoue et al., 2015; Miao et al., 2017). *TfxYl10A* with CBM2 might be responsible for removing the residual xylan attached to cellulose, thus clearing the way for cellulase action.

Xylanase application in biobleaching could remove the xylan cross-linking layer within pulp fibers, but require alkaline cooking at high temperature (Kumar et al., 2016; Talens-Perales et al., 2020). Thermostable and alkali-tolerant enzymes can also be advantageous for other industrial productions because the reactions can be performed at an elevated temperature and the structure of the enzymes is stabilized in these extreme conditions (Kumar et al., 2016; Mhiri et al., 2020; Zarafeta et al., 2020). *T. fusca* is a thermophilic actinobacterium that grows at 50–55°C and lives in a wide pH range from 4.0 to 10.0 (Lykidis et al., 2007). The optimal temperature of *TfxYl10A* is 80°C (Figure 2C) and the optimal pH of *TfxYl10A* is 9.0 (Figure 2D). The optimal temperature was higher than that of most fungal xylanases (40°C–70°C) (Polizeli et al., 2005). Of course, there are many natural xylanases with superior properties to *TfxYl10A*. For example, a thermophilic GH10 xylanase XynAF1 from the high-temperature composting strain *Aspergillus fumigatus* Z5 has optimal reaction temperature of 90°C and the

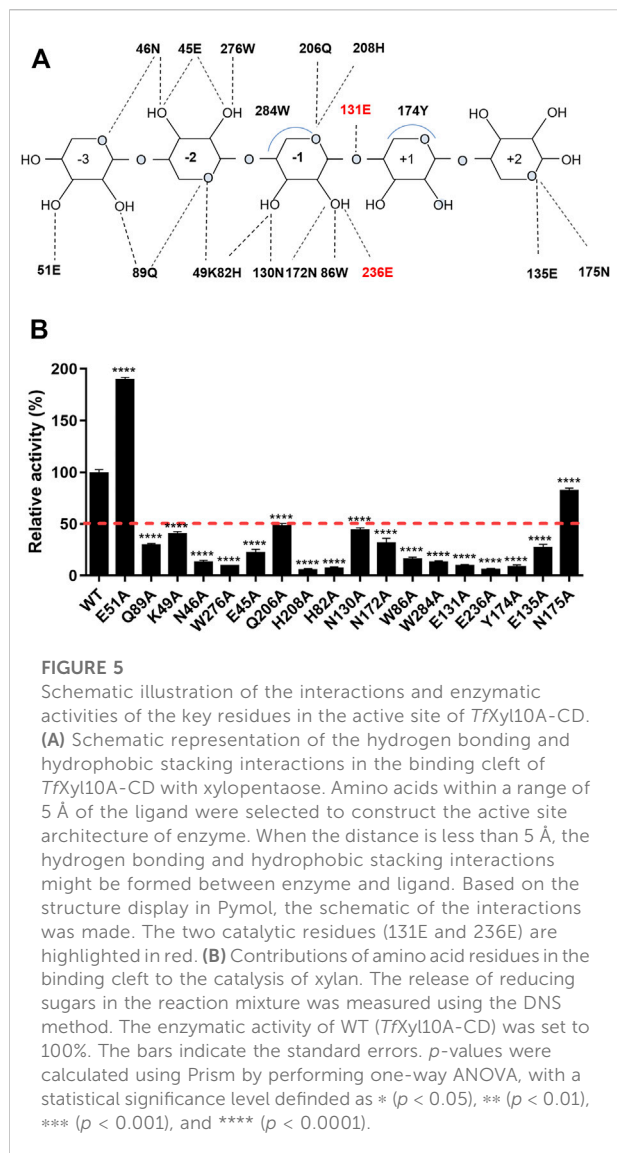


TABLE 1 Kinetic parameters of WT and the mutant E51A on BX.

Enzyme	K_m (mg/ml)	k_{cat} (1/s)	k_{cat}/K_m (mL* s ⁻¹ *mg ⁻¹)
WT	4.29 ± 0.39	169 ± 2	39.58 ± 3.22
E51A	16.35 ± 0.86**	581 ± 11***	35.58 ± 1.20 ^{ns}

P-values were calculated using Prism by performing one-way ANOVA, with a statistical significance level defined as ns (*p* > 0.05), * (*p* < 0.05), ** (*p* < 0.01), *** (*p* < 0.001), and **** (*p* < 0.0001).

thermostability of its mutant XynAF1-AC was increased by 6-fold through semi-rational design (Li et al., 2021). Xyn11 from *Pseudothermotoga thermarum* showed an excellent activity at 90°C and pH 10.5, and the fusion of CBM2 to Xyn11 enhanced the enzymatic activity under extreme conditions (Talens-Perales

et al., 2021). Therefore, the catalytic efficiency and thermostability of *Tfxyl10A* could be further improved by protein engineering. However, in this study, we found that the removal of CBM2 did not affect the optimal temperature and pH of the enzyme (Figures 2C,D), but it slightly increased the enzyme activity (Figure 3A). The removal of the linker had a great influence on both enzyme activity and thermal stability (Figures 2C, 3A). The linker region contains 9 Pro and 8 polar amino acids (2 Asp + 3 Glu + 2 Ser + 1 Thr), more than half of the total number of amino acids, which play an important role in structural stability (Talens-Perales et al., 2021). The deletion of the linker region may allow to deconstruct more easily the catalytic domain from the C-terminal under elevated temperatures. Previous studies have indicated that the linker length and flexibility play an important role in the activities of some cellulases, such as BsCel5A from *Bacillus subtilis* (Ruiz et al., 2016) and PoCel6A from *Penicillium oxalicum* (Gao et al., 2015). The linker region promotes enzyme activity and binding efficiency of LPMO towards polymeric substrate (Srivastava et al., 2022). In addition, Sonan et al. (2007) have reported that the linker region plays a key role in the cold adaptation of the a cellulase from an Antarctic bacterium.

Previous studies have compared the ligand-binding promiscuity and specificity of the main GH families by analyzing the active-site architecture (Liu et al., 2015; Tian et al., 2016). The active-site architecture analysis of the GH10 family revealed that 14 of 18 residues were well-conserved (conurf scores were “9”) across the active cleft (Figure 4D), which might be the most important for xylan degradation. Except for catalytic residues, conserved amino acids are mainly concentrated at the −2 and −1 subsites (Figure 4D). Interaction network analysis showed that the subsites −2 and −1 may provide main hydrogen-bonding for GH10 xylanases (Figure 5A). It was not surprising that most of the mutants had an impaired activity because the substrate-binding residues are relatively conserved and are important for enzyme functions. The amino acid residues located in the substrate active-site architecture of glycoside hydrolases, especially polar amino acids, and aromatic residues, played important roles in substrate recognition, catalysis, and products release (Chu et al., 2017; Yang and Han, 2018). Moreover, only one aromatic amino acid, Tyr, acted with xylose residues at the +1 subsite, which may be the structural basis for accommodating substituted xylose residues in this subsite, consistent with the previous analysis of the crystalline structure of GH10 xylanase (Pell et al., 2004). In another study, MeGlcA²Xyl₃ was the shortest side-chain hydrolysates for GH10 family xylanases, which also indicated the ability of +1 and −3 subsites on the xylanases to accommodate substituted xylose residues (Gong et al., 2016). Surprisingly, the relative activity of the mutant E51A at the −3 subsite was about 90% higher than that of the WT (Figure 5B). Although the catalytic efficiency (k_{cat}/K_m) of E51A was slightly lower than WT, the mutation of Glu reduced the binding force between enzyme and substrate. The enhancement of enzyme activity may be caused by the increase of product release rate. This was consistent with the results of

previous studies that manipulated the residues interacting with substrates in the distal regions could improve the activities of xylanases from GH11 families (Wu et al., 2018; Wu et al., 2020). To study the molecular mechanism underlying the catalytic promiscuity of *CbXyn10C*, Chu et al. (2017) found that Glu-52 at the -3 subsite had an important effect on enzyme activity, and mutation into many residues resulted in nearly doubled activity on cellulose with no significant change in xylanase activity.

To conclude, this study explored the function and molecular basis of a GH10 xylanase *TjXyl10A*, which was induced by a cellulose substrate. *TjXyl10A* is a thermostable and alkali-tolerant xylanase. *TjXyl10A* had a strong removal ability for substituted xylan residues attached to inner cellulose layers, and CBM2 could help *TjXyl10A* to bind to cellulose. These results suggested that *TjXyl10A* with CBM2 domain presented more advantages for industrial applications compared to the other enzymes. In addition, active-site architecture analysis and mutation experiments showed that the most important residues were centered on the -2 and -1 subsites near the cleavage site, whereas residues with moderate roles could be located at more distal regions of the binding cleft. Manipulating the amino acid residue at the distal -3 subsite of the active-site architecture of GH10 enzymes could improve their enzymatic activities. The results of this study not only identified an excellent candidate for bio-bleaching, but also provided guidance for the rational design and industrial application of xylanases belonging to the GH10 family. Further studies are required to create novel xylanases with higher thermal and alkali resistance and develop lignocellulosic hydrolysis methods to improve the efficiency of the catalytic process and increase techno-economic feasibility.

Data availability statement

The original contributions presented in the study are included in the article/Supplementary Material, further inquiries can be directed to the corresponding authors.

Author contributions

XW designed the experiments and wrote the manuscript. ZS and WT performed the experiments and analyzed the data. ML performed the bioinformatics analysis. SH modified the article.

References

- Ali, E., Araki, R., Zhao, G., Sakka, M., Karita, S., Kimura, T., et al. (2005). Functions of family-22 carbohydrate-binding modules in *Clostridium josui* Xyn10A. *Biosci. Biotechnol. Biochem.* 69 (12), 2389–2394. doi:10.1271/bbb.69.2389
- Boraston, A. B., Bolam, D. N., Gilbert, H. J., and Davies, G. J. (2004). Carbohydrate-binding modules: fine-tuning polysaccharide recognition. *Biochem. J.* 382, 769–781. doi:10.1042/bj20040892

XL, HY, and LW conceived the study design and edited the paper. All authors read and approved the final manuscript.

Funding

This study was funded by the Foundation of State Key Laboratory of Biobased Material and Green Papermaking, Qilu University of Technology, Shandong Academy of Sciences (grant number: GZKF202020), the Open Research Fund of State Key Laboratory of Biological Fermentation Engineering of Beer (grant number: K202005), and the Key Research and Develop Program of Shandong Province (No. 2020CXGC010601).

Acknowledgments

We thank International Science Editing (<http://www.internationalscienceediting.com>) for editing this manuscript.

Conflict of interest

The authors declare that the research was conducted in the absence of any commercial or financial relationships that could be construed as a potential conflict of interest.

Publisher's note

All claims expressed in this article are solely those of the authors and do not necessarily represent those of their affiliated organizations, or those of the publisher, the editors and the reviewers. Any product that may be evaluated in this article, or claim that may be made by its manufacturer, is not guaranteed or endorsed by the publisher.

Supplementary material

The Supplementary Material for this article can be found online at: <https://www.frontiersin.org/articles/10.3389/fbioe.2022.939550/full#supplementary-material>

- Bradford, M. M. (1976). A rapid and sensitive method for the quantitation of microgram quantities of protein utilizing the principle of protein-dye binding. *Anal. Biochem.* 72 (1), 248–254. doi:10.1016/0003-2697(76)90527-3

- Chen, S., and Wilson, D. B. (2007). Proteomic and transcriptomic analysis of extracellular proteins and mRNA levels in *Thermobifida fusca* grown on cellobiose and glucose. *J. Bacteriol.* 189 (17), 6260–6265. doi:10.1128/JB.00584-07

- Chu, Y., Tu, T., Penttinen, L., Xue, X., Wang, X., Yi, Z., et al. (2017). Insights into the roles of non-catalytic residues in the active site of a GH10 xylanase with activity on cellulose. *J. Biol. Chem.* 292 (47), 19315–19327. doi:10.1074/jbc.M117.807768
- Deng, Y., and Fong, S. S. (2010). Development and application of a PCR-targeted gene disruption method for studying CelR function in *Thermobifida fusca*. *Appl. Environ. Microbiol.* 76 (7), 2098–2106. doi:10.1128/AEM.02626-09
- Gao, L., Wang, L., Jiang, X., and Qu, Y. (2015). Linker length and flexibility induces new cellobiohydrolase activity of PoCel6A from *Penicillium oxalicum*. *Biotechnol. J.* 10 (6), 899–904. doi:10.1002/biot.201400734
- Gilbert, H. J., Knox, J. P., and Boraston, A. B. (2013). Advances in understanding the molecular basis of plant cell wall polysaccharide recognition by carbohydrate-binding modules. *Curr. Opin. Struct. Biol.* 23 (5), 669–677. doi:10.1016/j.sbi.2013.05.005
- Gomez del Pulgar, E. M., and Saadeddin, A. (2014). The cellulolytic system of *Thermobifida fusca*. *Crit. Rev. Microbiol.* 40 (3), 236–247. doi:10.3109/1040841X.2013.776512
- Gong, W., Zhang, H., Tian, L., Liu, S., Wu, X., Li, F., et al. (2016). Determination of the modes of action and synergies of xylanases by analysis of xylooligosaccharide profiles over time using fluorescence-assisted carbohydrate electrophoresis. *Electrophoresis* 37 (12), 1640–1650. doi:10.1002/elps.201600041
- Guillén, D., Sánchez, S., and Rodríguez-Sanoja, R. (2010). Carbohydrate-binding domains: multiplicity of biological roles. *Appl. Microbiol. Biotechnol.* 85 (5), 1241–1249. doi:10.1007/s00253-009-2331-y
- Gupta, G. K., Dixit, M., Kapoor, R. K., and Shukla, P. (2022). Xylanolytic enzymes in pulp and paper industry: new technologies and perspectives. *Mol. Biotechnol.* 64 (2), 130–143. doi:10.1007/s12033-021-00396-7
- Haim, A., Shiran, A., Eric, M., Ofer, C., Itay, M., Tal, P., et al. (2016). ConSurf 2016: an improved methodology to estimate and visualize evolutionary conservation in macromolecules. *Nucl. Acids Res.* 44 (W1), W344–W350. doi:10.1093/nar/gkw408
- Han, C., Liu, Y., Liu, M., Wang, S., and Wang, Q. (2020). Improving the thermostability of a thermostable endoglucanase from *Chaetomium thermophilum* by engineering the conserved noncatalytic residue and N-glycosylation site. *Int. J. Biol. Macromol.* 164, 3361–3368. doi:10.1016/j.ijbiomac.2020.08.225
- Herve, C., Rogowski, A., Blake, A. W., Marcus, S. E., Gilbert, H. J., and Knox, J. P. (2010). Carbohydrate-binding modules promote the enzymatic deconstruction of intact plant cell walls by targeting and proximity effects. *Proc. Natl. Acad. Sci. U. S. A.* 107 (34), 15293–15298. doi:10.1073/pnas.1005732107
- Inoue, H., Kishishita, S., Kumagai, A., Kataoka, M., Fujii, T., and Ishikawa, K. (2015). Contribution of a family 1 carbohydrate-binding module in thermostable glycoside hydrolase 10 xylanase from *Talaromyces cellulolyticus* toward synergistic enzymatic hydrolysis of lignocellulose. *Biotechnol. Biofuels* 8, 77. doi:10.1186/s13068-015-0259-2
- Khambhaty, Y., Akshaya, R., Rama Suganya, C., Sreeram, K. J., and Raghava Rao, J. (2018). A logical and sustainable approach towards bamboo pulp bleaching using xylanase from *Aspergillus nidulans*. *Int. J. Biol. Macromol.* 118, 452–459. doi:10.1016/j.ijbiomac.2018.06.100
- Khan, M. I. M., Sajjad, M., Sadaf, S., Zafar, R., Niazi, U. H. K., and Akhtar, M. W. (2013). The nature of the carbohydrate binding module determines the catalytic efficiency of xylanase Z of *Clostridium thermocellum*. *J. Biotechnol.* 168 (4), 403–408. doi:10.1016/j.jbiotec.2013.09.010
- Kim, J. H., Irwin, D., and Wilson, D. B. (2004). Purification and characterization of *Thermobifida fusca* xylanase 10B. *Can. J. Microbiol.* 50 (10), 835–843. doi:10.1139/w04-077
- Kittur, F. S., Mangala, S. L., Rus'd, A. A., Kitaoka, M., Tsujibo, H., and Hayashi, K. (2003). Fusion of family 2b carbohydrate-binding module increases the catalytic activity of a xylanase from *Thermotoga maritima* to soluble xylan. *FEBS Lett.* 549 (1–3), 147–151. doi:10.1016/s0014-5793(03)00803-2
- Kumar, S., Arumugam, N., Permaul, K., and Singh, S. (2016). Thermostable enzymes and their industrial applications. in *Microb. Biotechnol.: An Interdisciplinary Approach*. Editor P. Shukla (FL: CRC Press)115–162. doi:10.1201/9781315367880-6
- Kumar, V., Marin-Navarro, J., and Shukla, P. (2016). Thermostable microbial xylanases for pulp and paper industries: trends, applications and further perspectives. *World J. Microbiol. Biotechnol.* 32 (2), 34. doi:10.1007/s11274-015-2005-0
- Li, X., Han, C., Li, W., Chen, G., and Wang, L. (2020). Insights into the cellulose degradation mechanism of the thermophilic fungus *Chaetomium thermophilum* based on integrated functional omics. *Biotechnol. Biofuels* 13, 143. doi:10.1186/s13068-020-01783-z
- Li, G., Zhou, X., Li, Z., Liu, Y., Liu, D., Miao, Y., et al. (2021). Significantly improving the thermostability of a hyperthermophilic GH10 family xylanase XynAF1 by semi-rational design. *Appl. Microbiol. Biotechnol.* 105 (11), 4561–4576. doi:10.1007/s00253-021-11340-9
- Lin, X. Q., Han, S. Y., Zhang, N., Hu, H., Zheng, S. P., Ye, Y. R., et al. (2013). Bleach boosting effect of xylanase A from *Bacillus halodurans* C-125 in ECF bleaching of wheat straw pulp. *Enzyme Microb. Technol.* 52 (2), 91–98. doi:10.1016/j.enzmictec.2012.10.011
- Liu, S., Shao, S., Li, L., Cheng, Z., Tian, L., Gao, P., et al. (2015). Substrate-binding specificity of chitinase and chitosanase as revealed by active-site architecture analysis. *Carbohydr. Res.* 418, 50–56. doi:10.1016/j.carres.2015.10.002
- Lombard, V., Golaconda Ramulu, H., Drula, E., Coutinho, P. M., and Henrissat, B. (2013). The carbohydrate-active enzymes database (CAZy) in 2013. *Nucleic Acids Res.* 42 (D1), D490–D495. doi:10.1093/nar/gkt1178
- Ludwiczek, M. L., Heller, M., Kantner, T., and McIntosh, L. P. (2007). A secondary xylan-binding site enhances the catalytic activity of a single-domain family 11 glycoside hydrolase. *J. Mol. Biol.* 373 (2), 337–354. doi:10.1016/j.jmb.2007.07.057
- Lykidis, A., Mavromatis, K., Ivanova, N., Anderson, I., Land, M., DiBartolo, G., et al. (2007). Genome sequence and analysis of the soil cellulolytic actinomycete *Thermobifida fusca* YX. *J. Bacteriol.* 189 (6), 2477–2486. doi:10.1128/JB.01899-06
- Meng, D. D., Ying, Y., Chen, X. H., Lu, M., Ning, K., Wang, L. S., et al. (2015). Distinct roles for carbohydrate-binding modules of glycoside hydrolase 10 (GH10) and GH11 xylanases from *Caldicellulosiruptor* sp. strain F32 in thermostability and catalytic efficiency. *Appl. Environ. Microbiol.* 81 (6), 2006–2014. doi:10.1128/AEM.03677-14
- Mhiri, S., Bouanane-Darenfed, A., Jemli, S., Neifar, S., Ameri, R., Mezghani, M., et al. (2020). A thermophilic and thermostable xylanase from *Caldicoprobacter algeriensis*: Recombinant expression, characterization and application in paper biobleaching. *Int. J. Biol. Macromol.* 164, 808–817. doi:10.1016/j.ijbiomac.2020.07.162
- Miao, Y., Li, P., Li, G., Liu, D., Druzhinina, I. S., Kubicek, C. P., et al. (2017). Two degradation strategies for overcoming the recalcitrance of natural lignocellulosic xylan by polysaccharides-binding GH10 and GH11 xylanases of filamentous fungi. *Environ. Microbiol.* 19 (3), 1054–1064. doi:10.1111/1462-2920.13614
- Miller, G. L. (1959). Use of dinitrosalicylic acid reagent for determination of reducing sugar. *Anal. Chem.* 31 (3), 426–428. doi:10.1021/ac60147a030
- Morais, S., Barak, Y., Hadar, Y., Wilson, D. B., Shoham, Y., Lamed, R., et al. (2011). Assembly of xylanases into designer cellulosomes promotes efficient hydrolysis of the xylan component of a natural recalcitrant cellulosic substrate. *mBio* 2 (6), e00233–11. doi:10.1128/mBio.00233-11
- Motulsky, H. (2007). Prism 5 statistics guide. *GraphPad Softw.* 31, 39–42.
- Pell, G., Taylor, E. J., Gloster, T. M., Turkenburg, J. P., Fontes, C. M., Ferreira, L. M., et al. (2004). The mechanisms by which family 10 glycoside hydrolases bind decorated substrates. *J. Biol. Chem.* 279 (10), 9597–9605. doi:10.1074/jbc.M312278200
- Polizeli, M., Rizzatti, A., Monti, R., Terenzi, H., Jorge, J. A., and Amorim, D. (2005). Xylanases from fungi: properties and industrial applications. *Appl. Microbiol. Biotechnol.* 67 (5), 577–591. doi:10.1007/s00253-005-1904-7
- Pollet, A., Vandermarliere, E., Lammertyn, J., Strelkov, S. V., Delcour, J. A., and Courtin, C. M. (2009). Crystallographic and activity-based evidence for thumb flexibility and its relevance in glycoside hydrolase family 11 xylanases. *Proteins* 77 (2), 395–403. doi:10.1002/prot.22445
- Rencoret, J., Marques, G., Gutiérrez, A., Jiménez-Barbero, J., Martínez, Á. T., and del Río, J. C. (2013). Structural modifications of residual lignins from sisal and flax pulps during soda-AQ pulping and TCF/ECF bleaching. *Ind. Eng. Chem. Res.* 52 (13), 4695–4703. doi:10.1021/ie302810c
- Rio, D. C., Ares, M., Hannon, G. J., and Nilsen, T. W. (2010). Purification of RNA using TRIzol (TRI reagent). *Cold Spring Harb. Protoc.* 2010 (6), 5439–5445. doi:10.1101/pdb.prot5439
- Ruiz, D. M., Turowski, V. R., and Murakami, M. T. (2016). Effects of the linker region on the structure and function of modular GH5 cellulases. *Sci. Rep.* 6, 28504. doi:10.1038/srep28504
- Saleem, M., Tabassum, M. R., Yasmin, R., and Imran, M. (2009). Potential of xylanase from thermophilic *Bacillus* sp. XTR-10 in biobleaching of wood kraft pulp. *Int. Biodeterior. Biodegrad.* 63 (8), 1119–1124. doi:10.1016/j.ibiod.2009.09.009
- Shi, Z., Han, C., Zhang, X., Tian, L., and Wang, L. (2020). Novel synergistic mechanism for lignocellulose degradation by a thermophilic filamentous fungus and a thermophilic actinobacterium based on functional proteomics. *Front. Microbiol.* 11, 539438. doi:10.3389/fmicb.2020.539438
- Sonan, G. K., Receveur-Brechot, V., Duez, C., Aghajari, N., Czjzek, M., Haser, R., et al. (2007). The linker region plays a key role in the adaptation to cold of the cellulase from an Antarctic bacterium. *Biochem. J.* 407 (2), 293–302. doi:10.1042/bj20070640

- Srivastava, A., Nagar, P., Rathore, S., and Adlakha, N. (2022). The linker region promotes activity and binding efficiency of modular LPMO towards polymeric substrate. *Microbiol. Spectr.* 10 (1), e0269721. doi:10.1128/spectrum.02697-21
- Talens-Perales, D., Sanchez-Torres, P., Marin-Navarro, J., and Polaina, J. (2020). *In silico* screening and experimental analysis of family GH11 xylanases for applications under conditions of alkaline pH and high temperature. *Biotechnol. Biofuels* 13 (1), 198. doi:10.1186/s13068-020-01842-5
- Talens-Perales, D., Jimenez-Ortega, E., Sanchez-Torres, P., Sanz-Aparicio, J., and Polaina, J. (2021). Phylogenetic, functional and structural characterization of a GH10 xylanase active at extreme conditions of temperature and alkalinity. *Comput. Struct. Biotechnol. J.* 19, 2676–2686. doi:10.1016/j.csbj.2021.05.004
- Tian, L., Liu, S., Wang, S., and Wang, L. (2016). Ligand-binding specificity and promiscuity of the main lignocellulolytic enzyme families as revealed by active-site architecture analysis. *Sci. Rep.* 6, 23605. doi:10.1038/srep23605
- Walia, A., Guleria, S., Mehta, P., Chauhan, A., and Parkash, J. (2017). Microbial xylanases and their industrial application in pulp and paper biobleaching: a review. *3 Biotech.* 7 (1), 11. doi:10.1007/s13205-016-0584-6
- Wang, K., Cao, R., Wang, M., Lin, Q., Zhan, R., Xu, H., et al. (2019). A novel thermostable GH10 xylanase with activities on a wide variety of cellulosic substrates from a xylanolytic *Bacillus* strain exhibiting significant synergy with commercial celluclast 1.5 L in pretreated corn stover hydrolysis. *Biotechnol. Biofuels* 12, 48. doi:10.1186/s13068-019-1389-8
- Weiner, M. P., Costa, G. L., Schoettlin, W., Cline, J., Mathur, E., and Bauer, J. C. (1994). Site-directed mutagenesis of double-stranded DNA by the polymerase chain reaction. *Gene* 151 (1), 119–123. doi:10.1016/0378-1119(94)90641-6
- Wu, X., Tian, Z., Jiang, X., Zhang, Q., and Wang, L. (2018). Enhancement in catalytic activity of *Aspergillus niger* XynB by selective site-directed mutagenesis of active site amino acids. *Appl. Microbiol. Biotechnol.* 102 (1), 249–260. doi:10.1007/s00253-017-8607-8
- Wu, X., Zhang, S., Zhang, Q., Zhao, Y., Chen, G., Guo, W., et al. (2020). The contribution of specific subsites to catalytic activities in active site architecture of a GH11 xylanase. *Appl. Microbiol. Biotechnol.* 104 (20), 8735–8745. doi:10.1007/s00253-020-10865-9
- Yang, J., and Han, Z. (2018). Understanding the positional binding and substrate interaction of a highly thermostable GH10 xylanase from *Thermotoga maritima* by molecular docking. *Biomolecules* 8 (3), 64. doi:10.3390/biom8030064
- Yoo, C. G., Kim, H., Lu, F., Azarpira, A., Pan, X., Oh, K. K., et al. (2015). Understanding the physicochemical characteristics and the improved enzymatic saccharification of corn stover pretreated with aqueous and gaseous ammonia. *Bioenergy Res.* 9 (1), 67–76. doi:10.1007/s12155-015-9662-6
- Zarafeta, D., Galanopoulou, A. P., Leni, M. E., Kaili, S. I., Chegkazi, M. S., Chrysinia, E. D., et al. (2020). XynDZ5: a new thermostable GH10 xylanase. *Front. Microbiol.* 11, 545. doi:10.3389/fmicb.2020.00545
- Zhao, L., Geng, J., Guo, Y., Liao, X., Liu, X., Wu, R., et al. (2015). Expression of the *Thermobifida fusca* xylanase Xyn11A in *Pichia pastoris* and its characterization. *BMC Biotechnol.* 15, 18. doi:10.1186/s12896-015-0135-y
- Zheng, H., Liu, Y., Liu, X., Han, Y., Wang, J., and Lu, F. (2012). Overexpression of a *Paenibacillus campinasensis* xylanase in *Bacillus megaterium* and its applications to biobleaching of cotton stalk pulp and saccharification of recycled paper sludge. *Bioresour. Technol.* 125, 182–187. doi:10.1016/j.biortech.2012.08.101